공학석사학위논문

운용 조건을 고려한 태양광 추진 고고도 장기체공 항공기 날개의 다점 최적 설계

Multi-Point Design Optimization of HALE Wing Considering Operating Conditions

2013 년 2 월

서울대학교 대학원

기계항공공학부

최 선

운용 조건을 고려한 태양광 추진 고고도 장기체공 항공기 날개의 다점 최적 설계

Multi-Point Design Optimization of HALE Wing Considering Operating Conditions

지도교수 이 동 호

이 논문을 공학석사 학위논문으로 제출함

2012 년 12 월

서울대학교 대학원
기계항공공학부
최 선

최선의 공학석사 학위논문을 인준함

2012 년 12 월

위 원 장 : _____

부위원장 : _____

위 원 : _____

초 록

본 연구에서는 태양광 추진 고고도 장기체공 항공기 날개에 대해 운용 조건을 고려한 다점 최적설계를 수행 하였다. 해당 항공기의 임무 형상을 설계에 반영하여 전 임무 영역에서 요구 동력 및 날개의 변형을 최소화하였다. 최적설계를 위해 공력해석과 구조해석을 연계하여 두 결과가 수렴할 때까지 계산을 반복하였다. 3 차원 Euler equation 으로 공력 해석을 하였으며, 구조 해석은 UM/VABS 로 해석한 단면 해석 결과를 1 차원 보 해석에 반영하여 수행하였다. 설계 시 적용된 기저형상은 가장 긴 무인체공비행기록을 갖고 있는 QinetiQ 사 Zephyr 의 날개이다. 다목적 최적화 유전 알고리즘인 NSGA-II 를 이용하여 날개의 공력 및 구조 성능을 향상시켰고 이를 통해 항공기의 장기체공 능력을 보다 향상 시킬 수 있었다.

Key Words: High Altitude Long Endurance (HALE), Wing Design Optimization, Solar-UAV, NSGA-II, Aero-Structural Analysis

학 번: 2011-20760

Contents

Abstract..... Ⅰ

Contents..... Ⅱ

1. Introduction 1

1.1 Motivations.....1

1.2 Objective and Outline 3

2. Numerical and Design Method 5

2.1 Fluid-Structure Interaction(FSI) 5

2.1.1 Aerodynamic Analysis 7

2.1.2 Structural Analysis.....10

2.1.3 VMT Method 12

2.1.4 Displacement Transfer 13

2.2 Optimization Methodology.....14

2.2.1 Design of Experiment (DOE).....14

2.2.2 Artificial Neural Network 14

2.2.3 NSGA-II 16

2.2.4 Multi-Objective Optimization Method 18

3. Design Formulation 19

3.1 Design Variables and Design Space 19

3.2 Design Points and Design Objectives 20

3.3 Multidisciplinary Design Optimization 22

4. Design Results.....26

4.1 Pareto-Optimal Analysis.....26

4.2 Optimized Wing Shape.....28

5. Conclulsion.....31

References.....32

Abstract in Korean.....34

1. Introduction

1.1 Motivations

These days, energy cost has been increased due to energy consumption caused by industrial development. In addition, interest in alternative and renewable energy has grown as the world is facing climate change and global warming. Among them, research using solar energy as a power source of aircraft has been actively conducted since solar energy has small influence on environment and is possible to be used permanently.

Until now, about 90 kind of solar-powered aircrafts were developed after the first flight of 'Sunrise 1' with solar energy in 1974[1]. Since preliminary design of a S-HALE UAV was performed[2], detail multidisciplinary design optimization was conducted focused on energy balance[3]. On the other hand, QinetiQ's Zephyr established the world record for the longest duration, 14 days and 21 minutes, in 2010[4].

Solar Powered HALE aircraft has some characteristics. First of all, its wing has high aspect ratio and flexible wing structure because S-HALE requires high lift to drag ratio and light weight. Hence, large tip deflection up to 20% of span length occurs and fluid-structure coupling analysis is required to handle the phenomena. Secondly, solar-powered HALE conducts its mission going up and down like figure 1. This concept is to save energy. During daytime, the aircraft climbs to 23.62km to convert extra electric energy to potential energy. In contrast, the aircraft descends to 16.39km using potential

energy at night. Anyway, this causes a big difference in performances of S-HALE wing according to the flight condition.

Therefore, the multidisciplinary multi-point design optimization of S-HALE wing considering operating conditions is carried out in this study. The MDO introduced here uses the response surface methodology and high fidelity aero-structural analysis tool combining CFD and CSM.

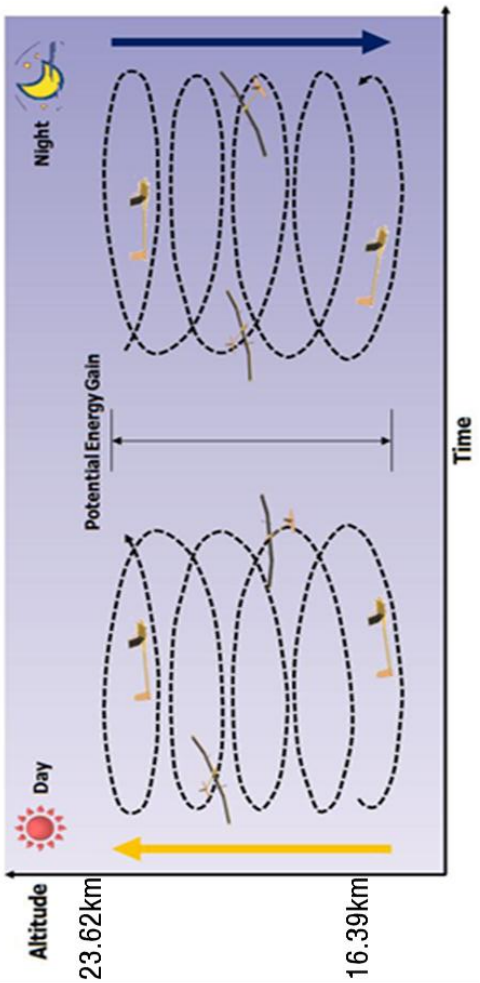

Figure 1. The Conceptual Flight Path [3]

1.2 Objective and Outline

In this study, optimized wing shape of S-HALE which has less required power and deflection at every design points than baseline is built. In addition, design points and design problem are defined referring the aircraft's mission profile.

3-D Euler equation was used to analyze aerodynamics of wing and drag was corrected with empirical equations. UM/VABS and 1-D beam code were adopted for structural analysis. Because of the high computational cost of aero-structural analysis, experimental points are extracted by 3k full factorial design method and Artificial Neural Network method constructed meta model. For the development MDO framework, NSGA-II which is able to deal with multi objective problem is chosen.

Taper ratio and span length are considered as design variables to minimize objectives, required power and deflection at design points. From the optimization results, taper ratio and span length for improved aerodynamic characteristics and better endurance performances.

The overall flowchart for design optimization is in figure 2.

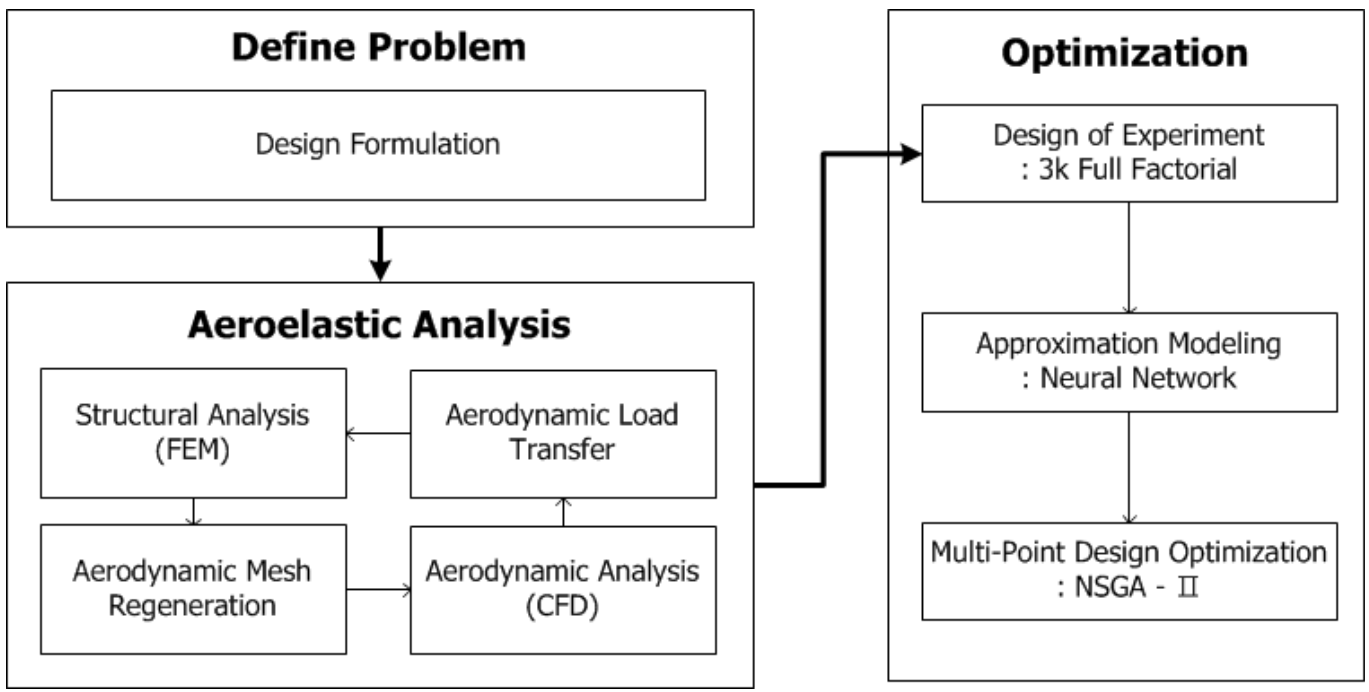

Figure 2. The Flow Chart for Design Optimization

2. Numerical and Design Method

2.1 Fluid-Structural Interaction (FSI)

The aerodynamic performance and the structural deformation of the wing are tightly coupled. The structural deformation of the wing changes the distribution of the aerodynamic force on the wing surface. And altered aerodynamic force distribution also has an influence on the structural deformation. Therefore, the accurate and efficient aeroelastic analysis of the wing plays an important role in the optimization process.

The way of coupling the aerodynamic analysis and structural analysis is as follows. First of all, deformed wing shape caused by its own weight is obtained by FEM. When performing wing structural analysis, the analysis is executed only focusing on the lift because the aerodynamic load works dominantly in the direction of lift. Second, CFD mesh newly covers the deformed shape of wing and is regenerated to calculate aerodynamic load. Next, aerodynamic analysis code calculates the converged aerodynamic force distribution. It is transformed to the structural nodal force and transferred to the FEM analysis. Then, structural analysis utilizing Nastran is performed again with those data. To achieve the converged wing deformation, the previous steps would be iteratively repeated about eight times. This method is defined as loosely coupling method and summarized in the flowchart (Figure 3).

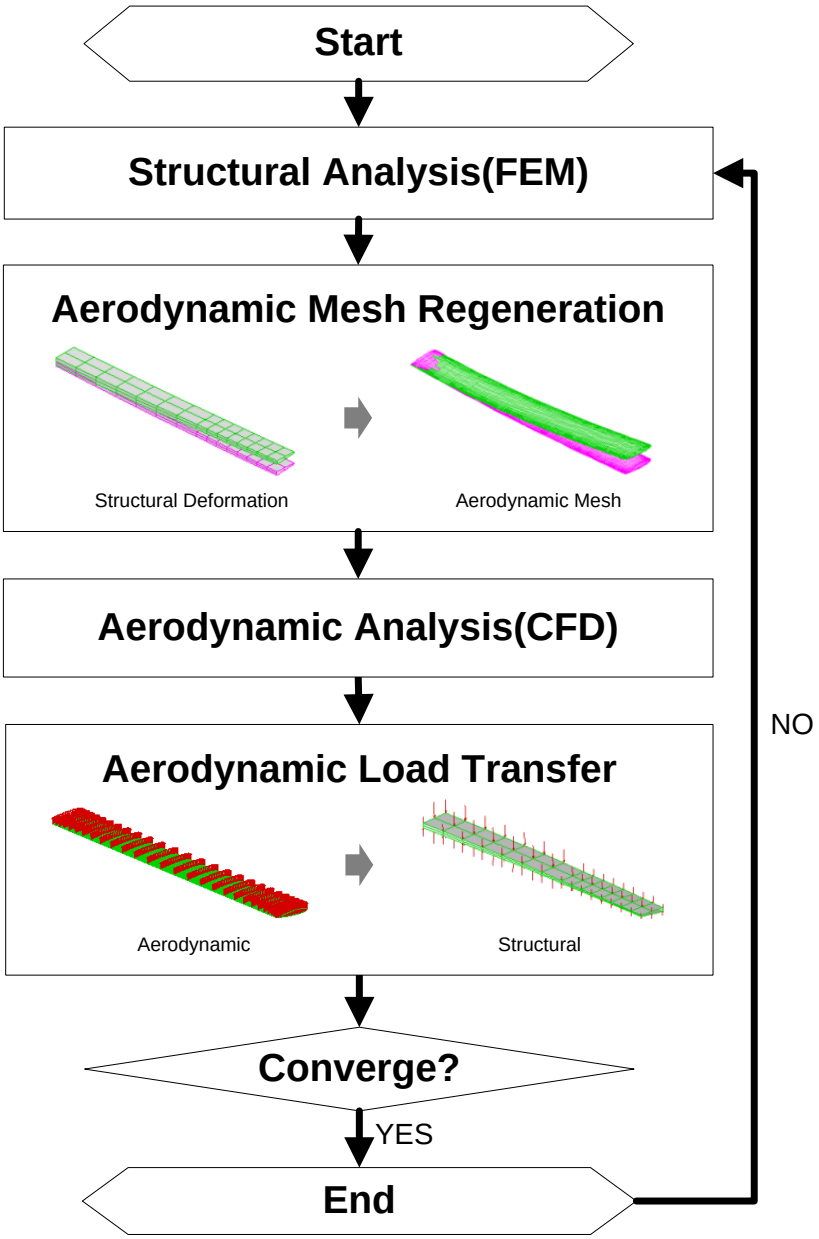

Figure 3. Flow Chart for Aero-Structural Analysis

2.1.1 Aerodynamic Analysis

A high fidelity CFD algorithm modeling the three-dimensional Euler equation is used to calculate the aerodynamics of the wing. The three-dimensional Euler equation can be written in the non-dimensionalized and conservative form as follows.

$$\frac{\partial Q}{\partial t} + \frac{\partial E}{\partial x} + \frac{\partial F}{\partial y} + \frac{\partial G}{\partial z} = 0 \tag{2.1}$$

$$Q = \begin{pmatrix} \rho \\ \rho u \\ \rho v \\ \rho w \\ \rho e \end{pmatrix}, E = \begin{pmatrix} \rho u \\ \rho u^2 + p \\ \rho uv \\ \rho uw \\ (\rho e + p)u \end{pmatrix}, F = \begin{pmatrix} \rho v \\ \rho uv \\ \rho v^2 + p \\ \rho vw \\ (\rho e + p)v \end{pmatrix}, G = \begin{pmatrix} \rho w \\ \rho uw \\ \rho vw \\ \rho w^2 + p \\ (\rho e + p)w \end{pmatrix} \tag{2.2}$$

In Eqs. (2.1) and (2.2), Q is the conservative variable vector and E, F and G are flux vectors. Also, ρ is the density and u, v and w are the velocity components in the direction of x, y and z-axis. e is the total specific energy and p is the pressure.

To discretize the computational domain, Upwind Method is used. And the time integration scheme adopted in this study is LU-SGS (Lower Upper Symmetric Gauss Seidel). In addition, Implicit Residual Smoothing scheme is introduced in order to accelerate the convergence of the numerical analysis and reduce the computational time[5].

Besides, the drag coefficient from Euler code is not accurate so it was corrected by empirical equations[6].

$$C_{D,profile} = 2.04 K_{dP} C_f \left(1 + \frac{0.38}{cos^2 \Lambda} C_L^2\right)$$
$$C_f = \frac{1.328}{\sqrt{Re}} \quad (Re < 5 \times 10^5) \tag{2.3}$$
$$K_{dP} = 1.25$$

Dae31 airfoil(Figure 4) was selected for cross-sectional shape of wing because it is well known for its outstanding performance at low Reynolds number range[7]. In addition, the O-H type volume grid is generated like figure 5 and 6. The number of mesh size is 121 along the airfoil surface, 33 along the spanwise direction and 94 normal to the wing surface.

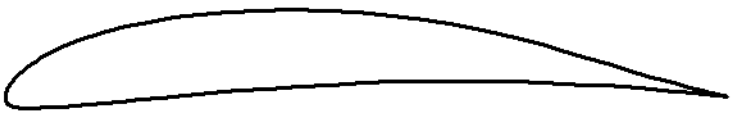

Figure 4. DAE31 Airfoil

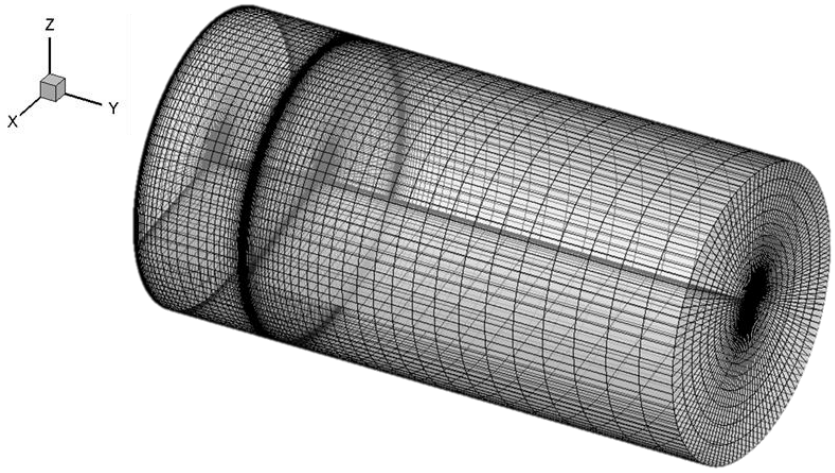

Figure 5. The O-H Type Volume Grid

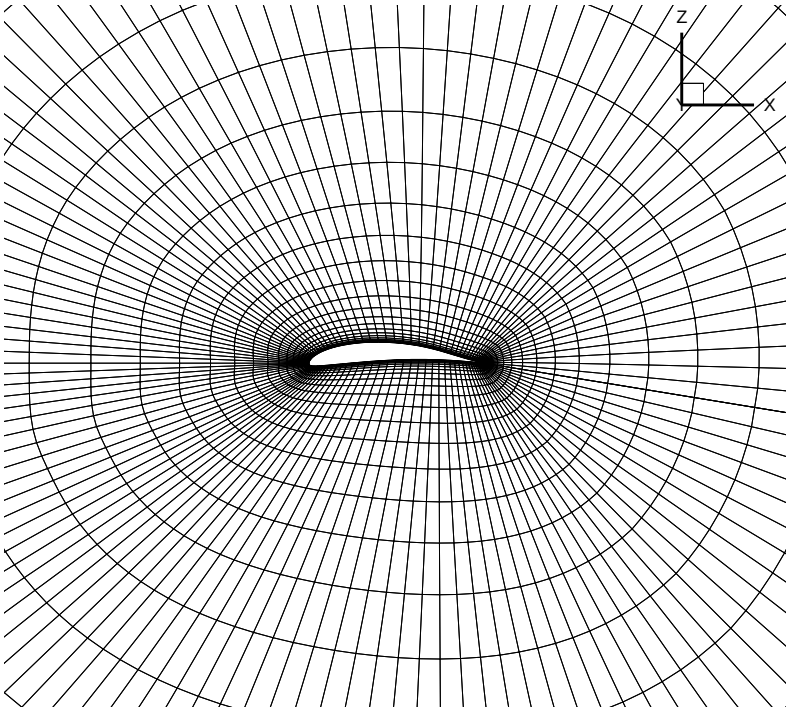

Figure 6. Plane View of Wing Root Section

2.1.2 Structural Analysis

The structural modeling process can be highly simplified through the dimensional reduction of the 3-D structure to a 1-D beam model. One can clearly distinguish two steps in a general beam theory: First, it comes the process of dimensional reduction, which is performed through a 2D analysis in the beam cross-sections; second, the computed equivalent stiffness and inertia properties are used in the 1-D analysis of the loaded beam[8].

- **UM / VABS**

UM/VABS is a FORTRAN90 code for computation of cross-sectional elastic, thermal, inertial and electric properties of active anisotropic beams. This code includes analysis using different beam theories: Euler-Bernoulli beam theory, Timoshenko beam theory, Vlasov beam theory and the original extended beam theory with finite section deformation modes. In all of these models, actuation effects of embedded active materials can be considered, as well as hygrothermal effects. Cross-sectional stress/strain, displacement can be computed for a full recovery of the 3-D electroelastic solution[9].

A cross-section model for structural analysis is in figure 7. The composite lamination is organized by cross-section optimization. The main spar and skin of the wing has eight and one layer, respectively. The material for spar is Graphite-Epoxy which is common for aircraft. On the other hand, very light material, Mylar, was applied for skin. Material properties are as follows.

T300/5208 Graphite-epoxy

: E_{11}=181 *GPa*, E_{22}=10.3 *GPa*, v_{12}=0.28, Mass density= 1,600 kg/m^3

Mylar, ply thickness: 0.2*mm*

: E =3.1 *GPa*, v =0.38, Mass density= 1,400 kg/m^3

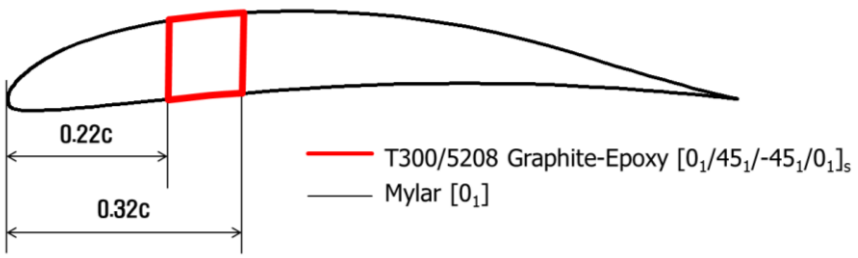

Figure 7. Cross-Sectional Model

2.1.3 VMT Method[10]

There is a great deal of complexity in the relation between CFD grid and FEM mesh. Because of inconsistency of aerodynamic grid and structural mesh, each result of analysis needs to be converted. Therefore, the VMT method is required to transfer lift distribution from CFD grid to FEM mesh.

Eq. (2.4) represents VMT method. V represents shear force, M for moment and T for Torque.

$$\begin{aligned} \sum_{i=1}^{N} f_i w_i &= a\sum_{i=1}^{N} f_i x_i + b\sum_{i=1}^{N} f_i y_i + c\sum_{i=1}^{N} f_i = V \\ \sum_{i=1}^{N} f_i w_i y_i &= a\sum_{i=1}^{N} f_i x_i y_i + b\sum_{i=1}^{N} y_i^2 + c\sum_{i=1}^{N} f_i y_i = M \\ \sum_{i=1}^{N} f_i w_i x_i &= a\sum_{i=1}^{N} f_i x_i^2 + b\sum_{i=1}^{N} f_i x_i y_i + c\sum_{i=1}^{N} f_i x_i = T \end{aligned} \tag{2.4}$$

x_i and y_i in Eq. (2.4) mean chordwise and spanwise nodal coordinate of the FEM mesh. VMT method is used to transfer aerodynamic load distribution into FEM mesh, satisfying the force equilibrium in each airfoil section. First of all, V, M and T are calculated by aerodynamic loads distribution. Next, weighting factor $w_i = ax + by + c$, or coefficients a, b, and c are calculated to satisfy the magnitude of each shear force, moment and torque calculated at aero node.

2.1.4 Displacement Transfer

There is a direct correlation between aerodynamic load and structural deformation. Aerodynamic load causes structural deformation, in contrast, structural deformation affects aerodynamic load. Thus, transferring displacement of deformed wing to aerodynamic grid is a necessary procedure. At this process, it is assumed that the geometry of airfoil is not change during deformation since the major deformation of the wing is due to bending and torsional behavior. Therefore, only the translations and rotations of airfoil are considered to create a deformed CFD mesh.

The deformed shape of wing in span direction is determined by the new location of airfoil. A displacement and rotational angle of cross section obtained by structural analysis were transferred and surface grid would be moved maintaining each shape of wing cross section. Finally, volume grid could be regenerated using moved surface grid.

2.2 Optimization Methodology

2.2.1 Design of Experiment (DOE)

Prior to creating an experimental design points, the allowable range of each of the n_v variables is defined by lower and upper bounds. For numerical stability and ease of notation, the range of each variable is scaled to [-1, 1]. The region enclosed by the lower and upper bounds on the variables is termed the design space. In this case, each of the n_v variables is specified at the lower bounds, midpoint and the upper bounds. Therefore, 3^{n_v} design points were created by this method.

At least $(n_v + 1)(n_v + 2) / 2$ response points are required to construct a response surface model which has n_v design variables. A 3k full factorial design method provides plenty response points to permit the estimation of the response surface model coefficients. However, as the number of design variable becomes large the evaluation of 3^{n_v} full factorial design becomes impractical. A full factorial design is used for ten or fewer design variables.

2.2.2 Artificial Neural Network

Artificial Neural Network (ANN) method was created based on the idea how human nervous system transfers and handles the information. It understands the behaviors of output variables by input variables and defines the relationship between the input variables and output variables in mathematical form. ANN has an advantage in representing the nonlinearity

of the complex system[12].

Generally, three-layer artificial neural network is commonly used and comprised of ‘input layer’, ‘hidden layer’ and ‘output layer’ as like figure 8. The number of neurons at input layer and output layer are same with the number of input variables and output variables. But the relationships between the number of neurons at hidden layer and the number of input variables or output variables are not clarified in this process.

If the number of neurons at hidden layer is not enough, the design points cannot be represented properly. On the other hand, the distortion may be occurred in the representation of the other design space by approximation model if the number is too many. As a result of various researches for this problem, it is generally applicable that the number of neurons at hidden layer is set as 1.5~2 times number of neurons at input layer to represent the design space properly.

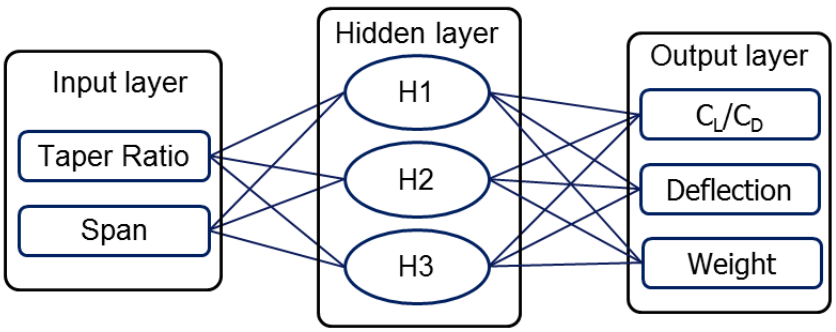

Figure 8. Artificial Neural Network

2.2.3 NSGA-Ⅱ

The NSGA-Ⅱ is the multi-objective optimization algorithm. The algorithm makes use of a fast non-dominated sorting approach to discriminate solutions, which is based on the concept of Pareto dominance and optimality.

The concept of Pareto dominance and optimality can be expressed as follows for a multi-objective minimization problem[13]:

$$\textbf{Minimize } f(x) = (f_1(x),\ f_2(x),\ \cdots, f_n(x))$$
$$\textbf{s.t. } g(x) = \big(g_1(x), g_2(x), \cdots, g_n(x)\big) \leq 0$$

where *f(x)* is the vector-valued function, *x* is the decision vector and *g(x)* is a vector of constraints.

Since NSGA-Ⅱ is a population-based algorithm, it starts with random generation of parent population, P_0, of potential solutions. The parent population, having size *N*, is checked for Pareto dominance and a fitness value equal to its nondomination level (i.e., 1 corresponds to the best non-domination level, 2 is the next best level, and so on) is assigned to each solution. The non-dominating sorting algorithm uses this fitness value to rank the solutions and assign them to the different fronts (i.e., each solution belongs to different fronts based on its domination level). The first front contains solutions that dominate solutions of all other fronts. An offspring

population, Q_0, of the same size as the parent population is created through recombination based on binary tournament selection and by inducing variations using mutation operators. After the initial generation, the procedure involves comparing the current population with previously identified non-dominated solutions. The crowded-comparison operator is the average distance between an individual solution and those solutions nearest to it in the objective space. It, therefore, represents the crowding distance, which is the largest cuboid enclosing that individual solution without including any other solution in the population[14].

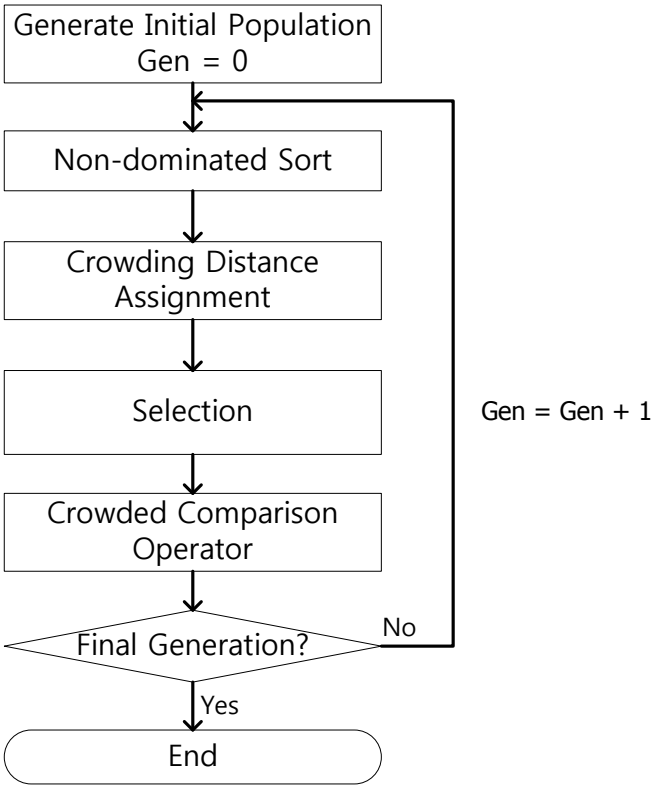

Figure 9. Procedure for NSGA-Ⅱ

2.2.4 Multi-Objective Optimization Method

Solving multi-objective scientific and engineering problem is a very difficult goal. There are some kinds of multi-objective optimization solution methods such as the weighted sum method, the ε -constraint method and the distance metric method[15, 16]. Among them, the distance metric method is adopted to construct the multi-objective function because the two objectives should be considered at the same time.

In the distance metric method, F^s is defined as follows:

$$F^s = (\sum_{1}^{n} |f_i(X) - \hat{f}_i|^p)^{\frac{1}{p}}$$

where $\hat{F} = [\hat{f}_1, \hat{f}_2, \cdots, \hat{f}_n]$ is a goal vector which is a predetermined vector by a user. The parameter p is usually 1, 2 or infinity. The function F^s measures distance from $F(X) = [f_1, f_2, \cdots, f_n]$ to $\hat{F} = [\hat{f}_1, \hat{f}_2, \cdots, \hat{f}_n]$. This method is sensitive to the position of $\hat{F}$.

3. Design Formulation

3.1 Design Variables and Design Space

The design space is consisted of parameters related to the planform of the wing. The number of design variables is two and the range of design variables are summarized in table 1. The taper ratio and span length are chosen as design variables by parametric study and they determine the wing planform. Here, the optimized wing shape of QinetiQ's Zephyr which has the world record for the longest duration by Park et al. is selected as the baseline of the optimization[3].

Table 1. Range of Design Variables

Design Variable	Minimum	Base	Maximum
Taper Ratio	0.5	1	1
Span	10.152	11.280	12.408

3.2 Design Points and Design Objectives

In general, a solar powered- HALE aircraft is maneuvered at several flight conditions like figure 10. The single-point design of the wing, which considers only one flight condition, has no significant meaning. Therefore, the multi-point design should be carried out taking the various flight conditions into account.

In this study, two representative flight conditions for solar-powered HALE aircraft and the requested design objectives at each flight condition are carefully selected and determined as follows;

First, the aircraft performs its mission like observation, surveillance, etc. at a low altitude(16.39*km*) during the daytime. Here, the largest deflection occur causing structural risk and performance degradation. Therefore, the deflection should be minimized to decrease decline of performance at a low altitude.

Second, the aircraft starts gliding and energy saving mode at night because there is no power source. Hence, the lower required power at a high altitude(23.62*km*) is favorable for long endurance.

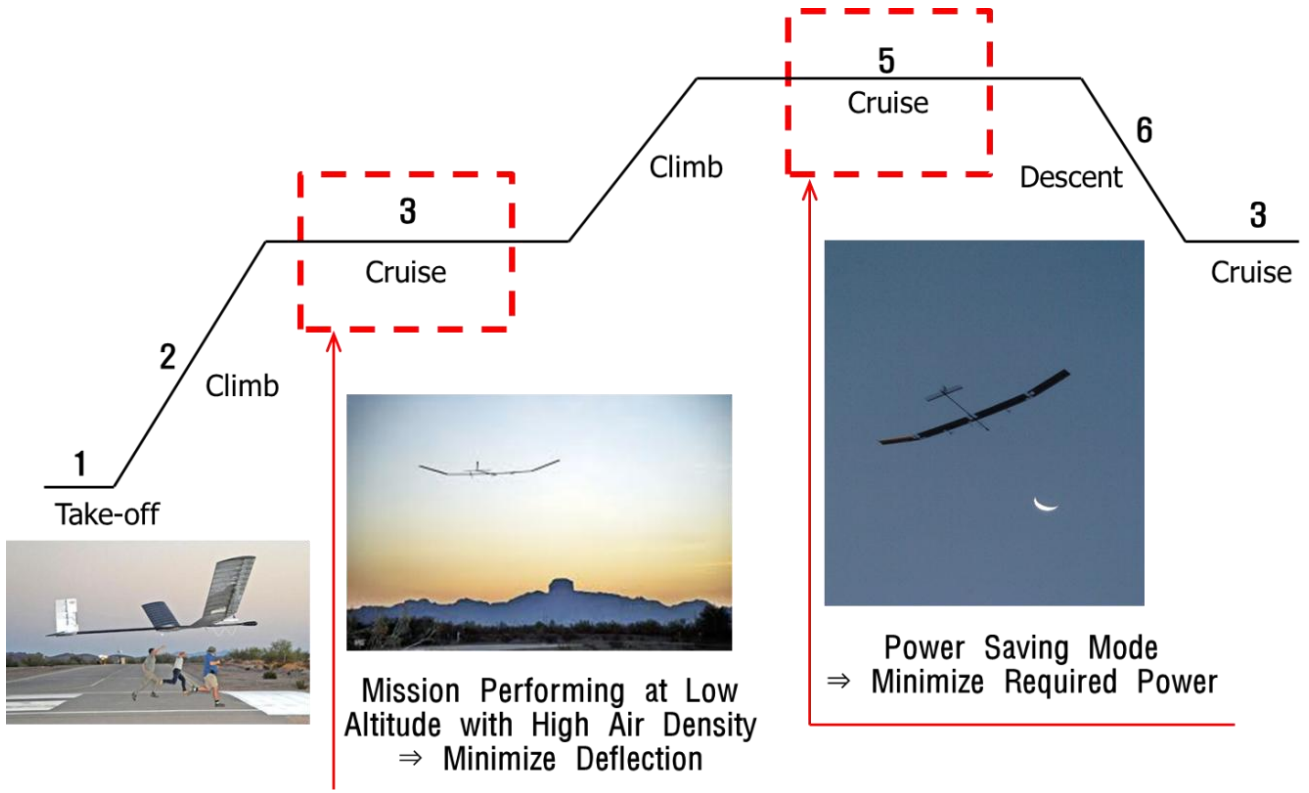

Figure 10. Mission Profile of S-HALE Aircraft

3.3 Multidisciplinary Design Optimization

Based on the static aeroelastic analysis coupling CFD and CSM, multi-point design optimization is performed. The multi-objective function and constraints used for the multi-point design optimization are defined as follow:

$$
\begin{aligned}
&\textit{Minimize} && \textit{Deflection at 16.39km} \\
& && \textit{Required Power at 23.62km} \\
&\textit{s.t.} && \textit{Wing Area} \geq 14.62\ m^2 \\
& && \textit{Required Power}_{base} \geq \textit{Required Power} \\
& && \textit{Deflection}_{base} \geq \textit{Deflection} \\
& && \textit{Lift} \geq \textit{Gross Weight}
\end{aligned}
$$

The subscript 'base' means that the values are the calculated result from the baseline wing. The deflection of the wing is calculated through the structural FEM code.

The minimal solar panel area which can produce enough energy for continuous flight is $14.62m^2$. On the other hand, the aerodynamic constraints are imposed on the required power to meet the goal that a design wing should have the aerodynamic performance at least as good as that of the baseline. The structural constraint means that the deflection of the optimized wing should be less than that of the baseline wing. Lastly, lift should be basically greater than gross weight.

- Construction of Response Surface Model

Nine numerical experimental points are selected through the 3k full factorial design method and the aeroelastic analysis is performed at the selected points. R^2_{adj} and the Root Mean Square Error (RMSE) are summarized in table 2. R^2_{adj} is larger than 0.99 for all response surface models and this guarantees the reliable prediction capability of the response surface models.

Table 2. Results of Regression Analysis

Y	RMSE	R^2
$Deflection_{16.39}$	0.0056	0.9995
$P_{req,\ 16.39}$	0.0138	0.9971
$Deflection_{20}$	0.0050	0.9996
$P_{req,\ 20}$	0.0135	0.9972
$Deflection_{23.62}$	0.0058	0.9995
$P_{req,\ 23.62}$	0.0133	0.9973
Gross Weight	0.0141	0.9970

The prediction profiles for the response surface models are illustrated in figure 11. Vertical axis means deflection and required power at each operating altitude. The prediction profiles are able to show the individual dependency or sensitivity of the response to the design variables. The range of each design variables is normalized to [-1, 1] and the responses are also normalized by the baseline values. As the slope is steeper, the response is more sensitive to the change of that design variable.

According to the prediction profiles, taper ratio has small influence on deflection. When taper ratio decreases, required power also decreases due to improved aerodynamic performances. In addition, required power decreases but deflection largely increases as span length increases.

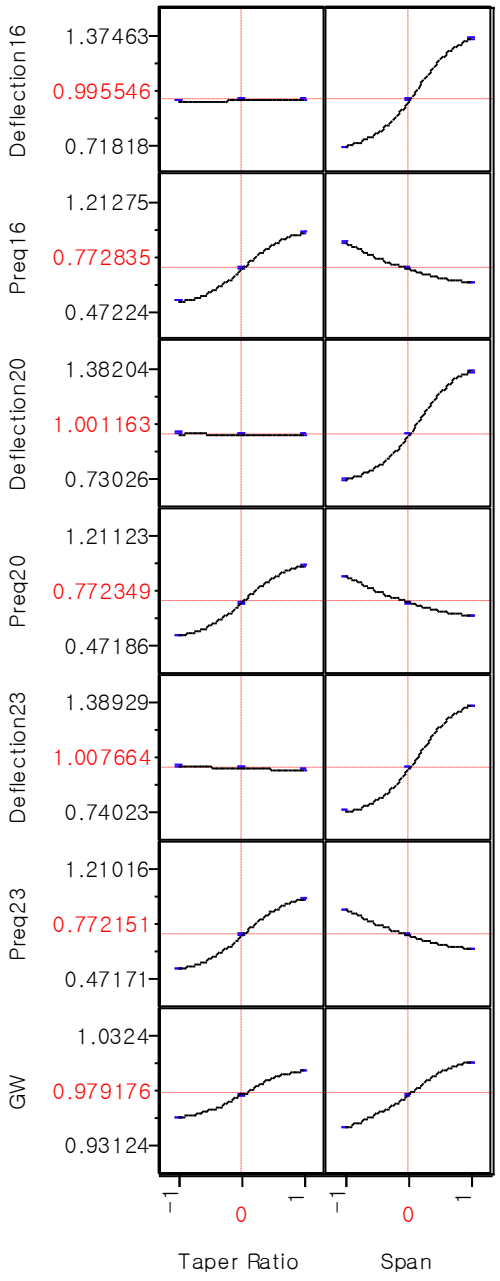

Figure 11. Prediction Profiles

4. Design Results

The multi-point design is investigated to improve the performances at each design points. The optimal wing is designed by minimizing objectives and the genetic optimizer controls this process. Required power and deflection are minimized and the endurance performances are improved equally at all design points and disciplines.

4.1 Pareto –Optimal Analysis

Figure 12 shows Pareto results. Among Pareto set, the optimum was selected considering required power at 23.62*km*, deflection at 16.39*km* and wing area.

First of all, wing area was considered to screen candidate solution set satisfying constraint. To obtain enough solar energy, the wing has to be larger than minimal area of solar cell, 14.62m^2. Therefore, the feasible region is upper-right side of the figure.

Then, two optimum points are chosen out of the feasible region using the distance metric method. Optimum Ⅰ is the point where the L_2 norm from utopia point is the least. And optimum Ⅱ has the minimum required power at 23.62*km* among candidate points.

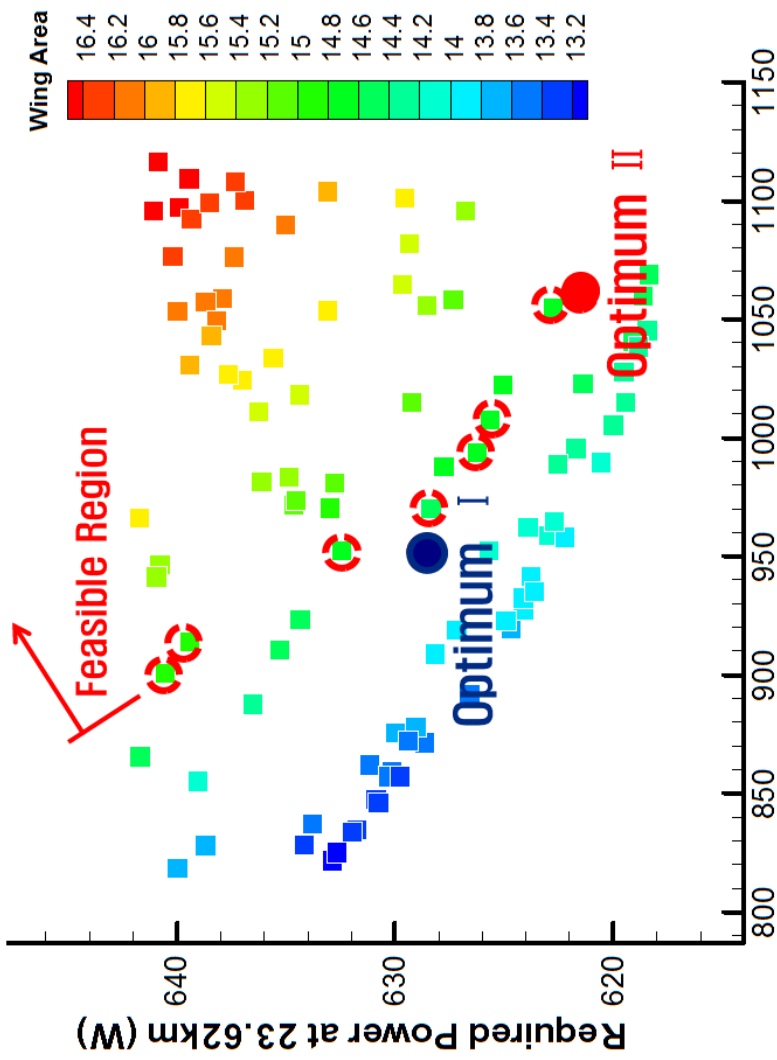

Figure 12. Pareto Results and Optimum Points

4.2 Optimized Wing Shape

The optimized wing and baseline are compared in figure 13 and the optimized design variables are summarized in table 3.

Optimum Ⅰ and Ⅱ have reduced taper ratio about 30%. The lift distribution of tapered wing follows elliptical lift distribution reducing induced drag. As a result, improved aerodynamic performance of tapered wing allows required power reduction. Furthermore, their span length have decreased to reduce deflection. Short span length is preferred in reducing deflection as span length works like moment arm. According to the optimization result, taper ratio is closely related to required power and deflection is mainly affected by span length.

The objectives and constraints of baseline and optimums are compared in table 4. Required power of optimum Ⅰ and Ⅱ are reduced and deflection has decreased also satisfying constraints.

Table 3. Optimized Design Variables

	Taper Ratio	Span
Baseline	1	11.28
Optimum 1	0.699 (30.1% ↓)	10.839 (3.91% ↓)
Optimum 2	0.649 (35.1% ↓)	11.143 (1.21% ↓)

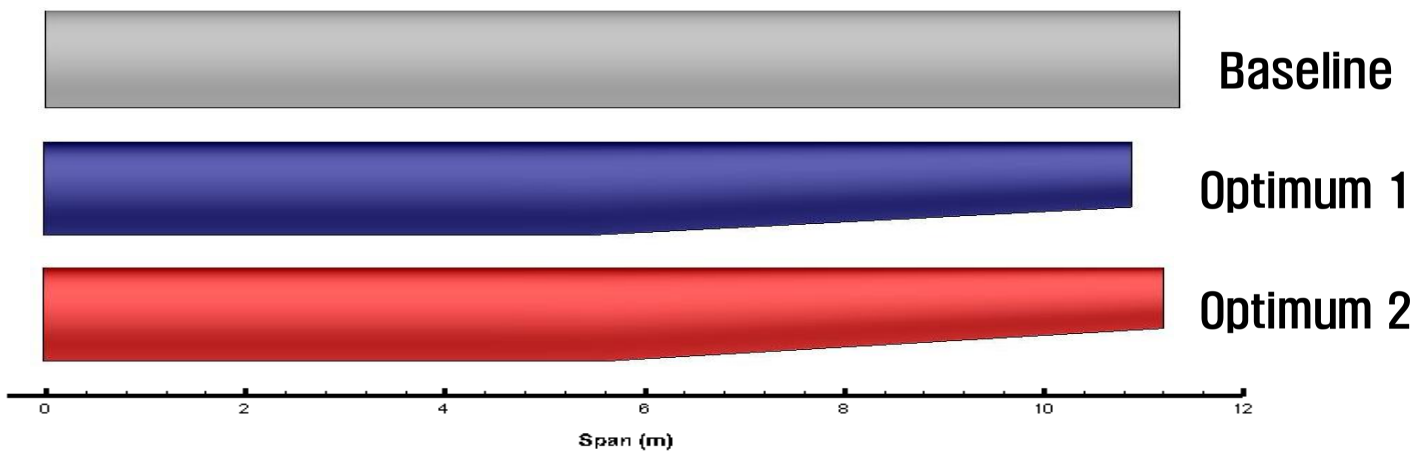

Figure 13. Optimized Result

Table 4. Objectives and Constraints

	Objectives		Constraints	
Case	Required $\text{Power}_{23.62\text{km}}$ (W)	$\text{Deflection}_{16.39\text{km}}$ (mm)	Wing Area (m^2)	$\text{Lift}_{23.62\text{km}}$ – Gross Weight (N)
Baseline	641.71	1118.76	16.69	152.02
Optimum 1	628.35 (2.08%↓)	969.95 (13.30%↓)	14.83	110.10
Optimum 2	621.56 (3.14%↓)	1060.29 (5.26%↓)	15.04	119.31

5. Conclusion

A multi-point design optimization has been performed for the S-HALE wing in this study. For Fluid-Structure Interaction (FSI) analysis, 3-D Euler code has been coupled with structural code separated into 2-D cross-sectional analysis and 1-D beam analysis. Also, NSGA- II is used to enhance the aero-structural performances at all design points. As a result, two optimums which have less required power and deflection than baseline are obtained by analyzing Pareto set.

In general, S-HALE conducts its mission going up and down to save extra solar energy during the daytime. Therefore, considering those operating conditions in design process is essential. Low altitude flight in the daytime and high altitude flight in the night are considered as representative design points.

According to the optimization process, influence of design variables on performances is confirmed. As taper ratio decreases, required power also decreases because of improved aerodynamic performance. On the other hand, short span length is favorable to reduce deflection.

References

[1] Andre Noth, “Design of Solar Powered Airplanes for Continuous Flight,” Ph. D. Dissertation, Technical Sciences, ETH ZURICH, 2008.

[2] Jon-Ahn, Nam-Hyo Kim and Sang-Chul Lee, “Preliminary Design of a Solar Powered HALE Airplane,” KSAS, Vol. 18, No. 2, pp.90-98, 1990.

[3] Kyung-Hyun Park, Sang-Gyu Min, Jon Ahn and Dong-Ho Lee, “Multidisciplinary Design Optimization(MDO) of a Medium-Sized Solar Powered HALE UAV Considering Energy Balancing,” KSAS, Vol. 40, No. 2, pp.129-138, 2012.

[4] Retrieved Jan. 27, 2013, from http://www.qinetiq.com

[5] Yu-Shin Kim, “Multidisciplinary Multi-Point Design Optimization of Supersonic Fighter Wing,” Ph. D. Dissertation, Department of Aerospace Engineering, Seoul National University, 2003.

[6] Sean Wakayama, “Lifting Surface Design Using Multidisciplinary Optimization,” Ph. D. Dissertation, Department of Aeronautics and Astronautics, Stanford University, 1994.

[7] J. Langford, “The Daedalus Project : A Summary of Lessons Learned”, AIAA/AHS/ASEE Aircraft Design, Systems and Operations Conference, AIAA 89-2048, 1989.

[8] Carlos Cesnik and Rafael Palacios, “UM/VABS Release 1.20 Theoretical Manual,” Active Aeroelasticity and Structures Research LAB, University of Michigan, May 2004.

[9] Carlos Cesnik and Rafael Palacios, “UM/VABS Release 1.23 User’s Manual,” Active Aeroelasticity and Structures Research LAB, University of Michigan, January 2005.

[10] JeongHwa Kim, YongJin Park, HyungMin Kang, Sangook Jun and Dong-Ho Lee, “FSI Analysis of HAR Wing at Low Speed Flight Condition,” International Conference on Computational Fluid Dynamics, Seoul, pp. 347-352, 2008.

[11] R. H. Meyers and D.C. Montgomery, “Response Surface Methodology: Process and Product Optimization Using Designed Experiments,” John Wiley & Sons,

1995.

[12] Sangook Jun, Yong-Hee Jeon, Joohyun Rho and Dong-ho Lee “Application of Collaborative Optimization Using Genetic Algorithm and Response Surface Method to an aircraft Wing Design,” Journal of Mechanical Science and Technology, Vol. 20, No. 1, pp.133-146, 2006.

[13] Veldhuizen, D. A. V. and Lamont, G. B., “Multiobjective evolutionary algorithms: analyzing the state-of-the-art”, Evolutionary Computation, Vol. 8, No. 2, pp.125-147, 2000.

[14] K Deb, A Pratap, S Agarwal and T Meyarivan, “A Fast and Elitist Multiobjective Genetic Algorithm:NSGA-II,” IEEE Transactions on Evolutionary Computation, Vol. 6, No. 2, pp.182-197, 2002.

[15] Eschenauer, H., Koski, J. and Osyczka, A., “Multicriteria Design Optimization,” Springer-Verlag, New York, 1990.

[16] Jung-Ho Lewe, “A Spotlight Search Method for Multi-criteria Optimization Problems,” 9th AIAA/ISSMO Symposium on Multidisciplinary Analysis and Optimization, AIAA-2002-5432, 2002.

Abstract

Multi-point design optimization of S-HALE wing is conducted considering its operating conditions. The mission profile of the aircraft is reflected to optimization process and required power and deflection in every operating condition are minimized. The aero-structural characteristics according to design variables are analyzed iteratively to optimize design. 3-D Euler equation is used as a governing equation to calculate aerodynamic properties. For structural analysis, UM/VABS compute cross-sectional properties and the results are applied to 1-D beam analysis. Baseline shape is wing of QinetiQ's Zephyr and it has the world record for the longest duration. Before the design optimization, parametric study of aeroelastic performance is performed to determine the design variables. The aerodynamic and structural performances are improved using the NSGA-II suitable for multi-objective design problem. From the results in this study, two optimized wing shape which have better endurance capability than baseline are obtained.

Key Words: High Altitude Long Endurance (HALE), Wing Design Optimization, Solar-UAV, NSGA-II, Aero-Structural Analysis

Student Number: 2011-20760